

Statistical properties of resonance widths for open Quantum Graphs

Tsampikos Kottos¹‡ and Holger Schanz²

¹Max-Planck-Institut für Strömungsforschung, Göttingen, Germany

²Institut für Nichtlineare Dynamik, Universität Göttingen, Germany

Abstract. We connect quantum compact graphs with infinite leads, and turn them into scattering systems. We derive an exact expression for the scattering matrix, and explain how it is related to the spectrum of the corresponding closed graph. The resulting expressions allow us to get a clear understanding of the phenomenon of resonance trapping due to over-critical coupling with the leads. Finally, we analyze the statistical properties of the resonance widths and compare our results with the predictions of Random Matrix Theory. Deviations appearing due to the dynamical nature of the system are pointed out and explained.

submitted to Waves in Random Media – special issue on Graphs

1. Introduction

Quantum graphs of one-dimensional wires connected at nodes were introduced already more than half a century ago to model physical systems. Depending on the envisaged application the precise formulation of the models can be quite diverse and ranges from solid-state applications to mathematical physics [1, 2, 3, 4, 5, 6, 7, 8, 9, 10, 11, 12]. Lately, quantum graphs attracted also the interest of the quantum chaos community because they can be viewed as typical and yet relatively simple examples for the large class of systems in which classically chaotic dynamics implies universal correlations in the semiclassical limit [13, 14, 15, 16, 17, 18, 19, 20, 21, 22]. Up to now we have only a limited understanding of the reasons for this universality, and quantum graph models provide a valuable opportunity for mathematically rigorous investigations of the phenomenon. In particular, for quantum graphs an exact trace formula exists [12, 13, 14] which is based on the periodic orbits of a mixing classical dynamical system. Moreover, it is possible to express two-point spectral correlation functions in terms of purely combinatorial problems [16, 17, 18, 19, 20] and to use this in order to investigate the origin of the connection between Random Matrix Theory (RMT) and the underlying classical chaotic dynamics.

By attaching infinite leads at the vertices, we get non-compact graphs, for which a scattering theory can be developed [23, 24, 25]. The quantum scattering matrix for such systems can be written explicitly, and the corresponding resonances can be calculated easily. It is the purpose of this paper to review their statistical properties and analyze their dependence on the boundary conditions that we impose at the vertices [26, 27, 28]. At the same time we apply the reaction-matrix formalism and for the first time we give a semiclassical interpretation of this theory in terms of the classical trajectories of the graph.

The paper is structured in the following way. In section 2, the mathematical model is introduced and the main definitions are given. Section 3 is devoted to the derivation of the scattering matrix for graphs. In section 4 we discuss the relation between the S-matrix of an open graph and the spectrum of the corresponding closed system (reaction-matrix formalism). The resonance width distribution for various types of graphs are presented and discussed in section 5 and deviations from RMT predictions [26, 27, 28] are analyzed. In the same section we also exhibit and analyze the phenomenon of resonance trapping occurring in specific graphs. Our conclusions are summarized in section 6.

2. Quantum Graphs: Definitions

We start by considering a *compact* graph \mathcal{G} . It consists of V *vertices* connected by B *bonds*. The number of bonds which emanate from each vertex i defines the valency v_i of the corresponding vertex (for simplicity we will allow only a single bond between any two vertices). The graph is called *v-regular* if all the vertices have the same

valency v . The total number of bonds is $B = \frac{1}{2} \sum_{i=1}^V v_i$. Associated to every graph is its connectivity matrix C . It is a square matrix of size V whose matrix elements $C_{i,j}$ take the values 1 if the vertices i, j are connected with a bond, or 0 otherwise. The bond connecting the vertices i and j is denoted by $b \equiv (i, j)$, and we use the convention that $i < j$. It will be sometimes convenient to use the “time reversed” notation, where the first index is the larger, and $\hat{b} \equiv (j, i)$ with $j > i$. We shall also use the directed bonds representation, in which b and \hat{b} are distinguished as two directed bonds conjugated by time-reversal. We associate the natural metric to the bonds, so that $x_{i,j}$ ($x_{j,i}$) measures the distance from the vertex i (j) along the bond. The length of the bonds are denoted by L_b and unless stated otherwise we shall assume that they are *rationally independent*. The mean length is defined by $\langle L \rangle \equiv (1/B) \sum_{b=1}^B L_b$ and in all numerical calculations below it will be taken to be 1. In the *directed-bond* notation $L_b = L_{\hat{b}}$. Finally, we define the total length of the graph $\mathcal{L} = \sum_{b=1}^B L_b$.

The *scattering* graph $\tilde{\mathcal{G}}$ is obtained by adding leads which extend from $M (\leq V)$ vertices to infinity. For simplicity we connect at most one lead to any vertex. The valency of these vertices increases to $\tilde{v}_i = v_i + 1$. The M leads are denoted by the index i of the vertex to which they are attached while x_i now measures the distance from the vertex along the lead i .

The Schrödinger operator (with $\hbar = 2m = 1$) is defined on the graph $\tilde{\mathcal{G}}$ in the following way: On the bonds b , the components Ψ_b of the total wave function Ψ are solutions of the one - dimensional equation

$$\left(-i \frac{d}{dx} - A_b\right)^2 \Psi_b(x) = k^2 \Psi_b(x), \quad b = (i, j) \quad (1)$$

where A_b (with $\Re e(A_b) \neq 0$ and $A_b = -A_{\hat{b}}$) is a “magnetic vector potential” which breaks the time reversal symmetry. In most applications we shall assume that all the A_b 's are equal and the bond index will be dropped. The components of the wave functions on the leads, $\Psi_i(x)$, are solutions of

$$-\frac{d^2}{dx^2} \Psi_i(x) = k^2 \Psi_i(x), \quad i = 1, \dots, M. \quad (2)$$

At the vertices, the wavefunction satisfies boundary conditions which ensure current conservation. To implement the boundary conditions, the components of the wave function on each of the bonds b and the leads i are expressed in terms of counter propagating waves with a wave-vector k :

$$\begin{aligned} \text{On the bonds : } \Psi_b &= a_b e^{i(k+A_b)x_b} + c_b e^{i(-k+A_b)x_b} \\ \text{On the leads : } \Psi_i &= I_i e^{-ikx_i} + O_i e^{ikx_i} . \end{aligned} \quad (3)$$

The amplitudes a_b, c_b on the bonds and I_i, O_i on the lead are related by

$$\begin{pmatrix} O_i \\ a_{i,j_1} \\ \vdots \\ a_{i,j_{v_i}} \end{pmatrix} = \Sigma^{(i)} \begin{pmatrix} I_i \\ c_{j_1,i} \\ \vdots \\ c_{j_{v_i},i} \end{pmatrix}, \quad \Sigma^{(i)} = \begin{pmatrix} \rho^{(i)} & \tau_{j_1}^{(i)} & \cdot & \tau_{j_{v_i}}^{(i)} \\ \tau_{j_1}^{(i)} & \tilde{\sigma}_{j_1,j_1}^{(i)} & \cdot & \tilde{\sigma}_{j_1,j_{v_i}}^{(i)} \\ \cdot & \cdot & \cdot & \cdot \\ \tau_{j_{v_i}}^{(i)} & \tilde{\sigma}_{j_{v_i},j_1}^{(i)} & \cdot & \tilde{\sigma}_{j_{v_i},j_{v_i}}^{(i)} \end{pmatrix}. \quad (4)$$

These equalities impose the boundary conditions at the vertices. The vertex scattering matrices $\Sigma_{j,j'}^{(i)}$, are $\tilde{v}_i \times \tilde{v}_i$ unitary symmetric matrices, and j, j' go over all the v_i bonds and the lead which emanate from i . The unitarity of $\Sigma^{(i)}$ guarantees current conservation at each vertex.

On the right hand side of (4), the vertex scattering matrix $\Sigma^{(i)}$ was written explicitly in terms of the vertex reflection amplitude $\rho^{(i)}$, the lead-bond transmission amplitudes $\{\tau_j^{(i)}\}$, and the $v_i \times v_i$ bond-bond transition matrix $\tilde{\sigma}_{j,j'}^{(i)}$, which is *sub unitary* ($|\det \tilde{\sigma}^{(i)}| < 1$), due to the coupling to the leads. Vertices which are not coupled to leads have $\rho^{(i)} = 1$, $\tau_j^{(i)} = 0$, while the bond-bond transition matrix $\tilde{\sigma}_{j,j'}^{(i)}$ is unitary.

Graphs for which there are no further requirements on the $\Sigma^{(i)}$ shall be referred to as *generic*. In this case the vertex scattering matrices $\Sigma^{(i)}$ are chosen from the ensemble of unitary symmetric $\tilde{v}_i \times \tilde{v}_i$ random matrices, as explained in [19]. However, often it is more convenient to compute the vertex scattering matrices from the requirement that the wave function is continuous and satisfies current conservation at all vertices [13, 14]. In this case the resulting $\tilde{\Sigma}^{(i)}$ matrices read [23]:

$$\tilde{\sigma}_{j,j'}^{(i)} = \frac{(1 + e^{-i\omega_i})}{\tilde{v}} - \delta_{j,j'}; \quad \tau_j^{(i)} = \frac{(1 + e^{-i\omega_i})}{\tilde{v}}; \quad \rho^{(i)} = \frac{(1 + e^{-i\omega_i})}{\tilde{v}} - 1 \quad (5)$$

where $\omega_i = 2 \arctan \frac{\lambda_i}{\tilde{v}_i k}$. The parameters $0 \leq \lambda_i \leq \infty$ are free parameters which determine the boundary conditions. We shall refer to the λ_i as the *vertex scattering potential*. The special case of zero λ_i corresponds to Neumann boundary conditions. Dirichlet boundary conditions result from $\lambda_i = \infty$. A finite value of λ_i introduces a new length scale. It is natural therefore, to interpret it in physical terms as a representation of a local impurity or an external fields [29]. We finally note that the above model can be considered as a generalization of the Kronig-Penney model to a multiply connected, yet one dimensional manifold.

3. The S-matrix for Quantum Graphs

It is convenient to discuss first graphs with leads connected to all the vertices $M = V$. The generalization to an arbitrarily number $M \leq V$ of leads (channels) is straightforward and will be presented at the end of this section.

To derive the scattering matrix, we first write the bond wave functions using the two representations which are conjugated by “time reversal”:

$$\begin{aligned} \Psi_b(x_b) &= a_b e^{i(k+A_b)x_b} + c_b e^{i(-k+A_b)x_b} = \\ \Psi_{\hat{b}}(x_{\hat{b}}) &= a_{\hat{b}} e^{i(k+A_{\hat{b}})x_{\hat{b}}} + c_{\hat{b}} e^{i(-k+A_{\hat{b}})x_{\hat{b}}} = \\ &= a_{\hat{b}} e^{i(-k-A_{\hat{b}})x_b} e^{i(k+A_{\hat{b}})L_b} + c_{\hat{b}} e^{i(-k+A_{\hat{b}})L_b} e^{i(k-A_{\hat{b}})x_b} . \end{aligned} \quad (6)$$

Hence,

$$c_b = a_{\hat{b}} e^{i(k+A_{\hat{b}})L_b}, \quad a_b = c_{\hat{b}} e^{i(-k+A_{\hat{b}})L_b}. \quad (7)$$

In other words, but for a phase factor, the outgoing wave from the vertex i in the direction j is identical to the incoming wave at j coming from i .

Substituting a_b from Eq. (7) in Eq. (4), and solving for $c_{i,j}$ we get

$$\begin{aligned} c_{i,j'} &= \sum_{r,s} \left(\mathbf{1} - \tilde{S}_B(k; A) \right)_{(i,r),(s,j)}^{-1} D_{(s,j)} \tau_s^{(j)} I_j \\ O_i &= \rho^{(i)} I_i + \sum_{j'} \tau_{j'}^{(i)} c_{ij'} \end{aligned} \quad (8)$$

where $\mathbf{1}$ is the $2B \times 2B$ unit matrix. Here, the ‘‘bond scattering matrix’’ \tilde{S}_b is a sub-unitary matrix in the $2B$ dimensional space of directed bonds which propagates the wavefunctions. It is defined as $\tilde{S}_B(k, A) = D(k; A)\tilde{R}$, with

$$\begin{aligned} D_{ij,i'j'}(k, A) &= \delta_{i,i'} \delta_{j,j'} e^{ikL_{ij} + iA_{i,j}L_{ij}} \\ \tilde{R}_{ji, nm} &= \delta_{n,i} C_{j,i} C_{i,m} \tilde{\sigma}_{ji, im}^{(i)}. \end{aligned} \quad (9)$$

$D(k, A)$ is a diagonal unitary matrix which depends only on the metric properties of the graph, and provides a phase which is due to free propagation on the bonds. The sub-unitary matrix \tilde{R} depends on the connectivity and on the bond-bond transition matrices $\tilde{\sigma}$. It assigns a scattering amplitude for transitions between connected directed bonds. \tilde{R} is sub-unitary, since

$$|\det \tilde{R}| = \prod_{i=1}^V |\det \tilde{\sigma}^{(i)}| < 1. \quad (10)$$

Replacing $c_{i,j'}$ in the second of Eqs. (8) we get the following relation between the outgoing and incoming amplitudes O_i and I_j on the leads:

$$O_i = \rho^{(i)} I_i + \sum_{j'rs} \tau_{j'}^{(i)} \left(\mathbf{1} - \tilde{S}_B(k; A) \right)_{(i,r),(s,j)}^{-1} D_{(s,j)} \tau_s^{(j)} I_j. \quad (11)$$

Combining (11) for all leads $i = 1, \dots, V$, we obtain the unitary $V \times V$ scattering matrix $S^{(V)}$,

$$S_{i,j}^{(V)} = \delta_{i,j} \rho^{(i)} + \sum_{r,s} \tau_r^{(i)} \left(\mathbf{1} - \tilde{S}_B(k; A) \right)_{(i,r),(s,j)}^{-1} D_{(s,j)} \tau_s^{(j)}. \quad (12)$$

Finally, a multiple scattering expansion for the S -matrix is obtained by substituting

$$\left(\mathbf{1} - \tilde{S}_B(k; A) \right)^{-1} = \sum_{n=0}^{\infty} \tilde{S}_B^n(k; A) \quad (13)$$

into Eq. (12). The expansion (13) converges absolutely on the real k -axis since for generic graphs the spectrum of \tilde{S} is strictly inside the unit circle (or else, for $k + i\epsilon$, with $\epsilon > 0$ arbitrarily small).

The scattering matrix can be decomposed into two parts $S^{(V)}(k) = \langle S^{(V)} \rangle_k + S^{fl}(k)$ which are associated with two well separated time scales of the scattering process. $\langle S^{(V)} \rangle_k$ can be evaluated by averaging term by term the S -matrix resulting from the substitution of the multiple scattering expansion (13) in (12). Since all terms, but for the prompt reflections, are oscillatory functions of k , they average to zero (we assume that the k -window over which the averaging is performed is sufficiently large i.e. larger than $2\pi/L_{\min}$) and thus we get that $\langle S^{(V)} \rangle_k = S^D = \delta_{i,j} \rho^{(i)}$. The fluctuating component of the S matrix, $S^{fl}(k)$, starts by a transmission from the incoming lead i to the bonds

(i, r) with transmission amplitudes $\tau_r^{(i)}$. The wave gains a phase $e^{i(k+A_b)L_b}$ for each bond it traverses and a scattering amplitude $\tilde{\sigma}_{r,s}^{(i)}$ at each vertex. Eventually the wave is transmitted from the bond (s, j) to the lead j with an amplitude $\tau_s^{(j)}$. Explicitly,

$$S_{i,j}^{(V)} = \delta_{i,j}\rho^{(i)} + \sum_{t \in \mathcal{T}_{i \rightarrow j}} \mathcal{B}_t e^{i(kl_t + \Theta_t)} \quad (14)$$

where $\mathcal{T}_{i \rightarrow j}$ is the set of the trajectories on $\tilde{\mathcal{G}}$ which lead from i to j . \mathcal{B}_t is the amplitude corresponding to a path t and is given by the product of all vertex-scattering matrix elements encountered along t . Length and directed length of the path are $l_t = \sum_{b \in t} L_b$ and $\Theta_t = \sum_{b \in t} L_b A_b$, respectively. Thus the scattering amplitude $S_{i,j}^{(V)}$ is a sum of a large number of partial amplitudes, whose complex interference brings about the typical irregular fluctuations of $|S_{i,j}^{(V)}|^2$ as a function of k .

We finally comment that the formalism above can be easily modified for graphs where not all the vertices are attached to leads. If the vertex l is not attached, one has to set $\rho^{(l)} = 1, \tau_j^{(l)} = 0$ in the definition of $\Sigma^{(l)}$. The dimension of the scattering matrix is then changed accordingly.

4. Relations between spectrum and S-matrix

4.1. Secular equation

There exists an intimate link between the scattering matrix and the spectrum of the corresponding closed graph. It manifests the exterior-interior duality for graphs [13, 23]. The spectrum of the closed graph is the set of wave-numbers for which $S^{(V)}$ has +1 as an eigenvalue. This corresponds to a solution where no currents flow in the leads so that the conservation of current is satisfied on the internal bonds. 1 is in the spectrum of $S^{(V)}$ if

$$\zeta_{\mathcal{G}}(k) = \det[\mathbf{1} - S^{(V)}(k)] = 0 \quad . \quad (15)$$

Eq. (15) can be transformed in an alternative form

$$\zeta_{\mathcal{G}}(k) = \det[\mathbf{1} - \rho] \frac{\det[\mathbf{1} - D(k)R]}{\det[\mathbf{1} - D(k)\tilde{R}]} = 0 \quad ; \quad R_{i,r;s,j} = \tilde{R}_{i,r;s,j} + \delta_{r,s} \frac{\tau_i^{(r)} \tau_j^{(r)}}{1 - \rho^{(r)}}. \quad (16)$$

which is satisfied once

$$\det[\mathbf{1} - D(k)R] = 0. \quad (17)$$

In contrast to \tilde{R} , R is a unitary matrix in the space of directed bonds, and therefore the spectrum is real. Eq. (17) is the secular equation for the spectrum of the compact part of the graph [13, 14, 23].

4.2. Reaction-matrix formalism

Eq. (15) allows to compute the spectrum of the closed graph from the S -matrix of the open graph. This relation can be inverted: it is possible to express the S -matrix at an arbitrary wavenumber k in terms of all eigenvalues and eigenfunctions of the

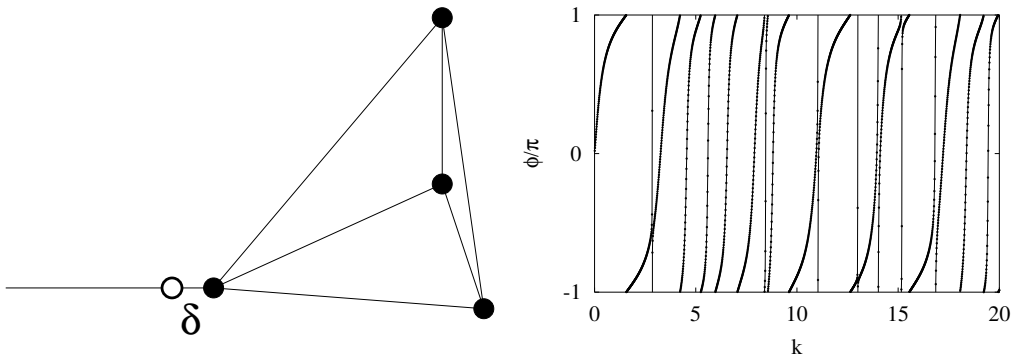


Figure 1. A tetrahedron with a single attached scattering channel (left) is used to illustrate the reaction-matrix theory for graphs. The empty circle shows an auxiliary vertex with Neumann b. c. which is used for the derivation of Eq. 20. On the right we compare the exact phase of the S-matrix of this graph (full line) to an approximation computed with the help of Eqs. (18), (21) from the lowest 500 eigenstates of the graph (dots).

corresponding closed graph. This is achieved by applying to quantum graphs methods which were developed in the context of nuclear physics: Wigner and Eisenbud [30] introduced in the late forties the reaction matrix as a connecting element between a closed and the corresponding scattering system. The projection-operator formalism of Feshbach [31] allows a systematic separation of the Hilbert space of a closed system from the embedding scattering system and on this basis Weidenmüller and coworkers developed a theory expressing the S-matrix in terms of an effective non-Hermitian Hamiltonian [32] which contains the dynamics of the closed system and the coupling to the scattering channels. This effective Hamiltonian is the basis for the RMT results on resonance statistics that we will discuss in the following sections, and therefore it is important to understand how reaction-matrix theory and Weidenmüller approach work in quantum graphs.

In order to achieve this understanding we consider first the Green's function G of a *closed* graph. It can be defined by the infinite spectral sum

$$G(x_b, x_{b'}; k) = \sum_{n=1}^{\infty} \frac{\Phi_n(x_b)\Phi_n^*(x_{b'})}{k^2 - k_n^2}, \quad (18)$$

where k_n denote the n th eigenvalue and $\Phi_n(x_b)$ the corresponding eigenfunction at distance x_b at the bond b . The graph will later be opened by attaching leads to the vertices $1 \leq j \leq M$ on which we assume Neumann boundary conditions (the b. c. at other vertices are arbitrary). We denote by $G_{jj'}$ the values of the Green's function on these vertices and introduce the Hermitian *reaction matrix*

$$K_{jj'} = k G_{jj'}. \quad (19)$$

We will show that K is related to the S-matrix via

$$K = -\mathbf{1}(I - S)^{-1}(I + S), \quad (20)$$

which is equivalent to

$$S = -(I + \mathbf{1}K)^{-1}(I - \mathbf{1}K). \quad (21)$$

For technical reasons it is easier to derive Eqs. (20), (21) in a situation where the leads are attached to vertices j with valency $v_j = 1$ and Neumann b. c. An example is shown in Fig. 1. As long as we consider Neumann b. c. this is no restriction of generality since the length δ of the bond reaching a "dead end" at vertex j in the closed graph can be arbitrarily small, and it can easily be shown that in the limit $\delta \rightarrow 0$ spectrum and eigenfunctions of the graphs with and without the attached arm coincide. Hence, after Eq. (20) is established with the help of auxiliary vertices, these vertices can be disregarded. Note that due to this construction $\rho^{(j)}$ in Eqs. (12), (14) is zero: in the scattering system the vertices to which the leads are formally attached have perfect transmission and are effectively absent.

There are two independent ways to arrive at Eqs. (20), (21). The first simply repeats the corresponding arguments for billiard systems [33, 34]. In fact the case of a quantum graph is completely equivalent up to the additional simplification that the attached leads do not allow for multiple transversal modes. However, here we will follow a different route which is more specific to quantum graphs as it relies on the exact representation of the corresponding S-matrix as a sum over classical trajectories (see Eq. (14)). There is a similar expansion of the Green's function in terms of classical trajectories

$$G(x, x'; k) = \frac{1}{2ik} \sum_{t: x' \rightarrow x} \mathcal{B}_t e^{i(kl_t + \Theta_t)}, \quad (22)$$

where t denotes a trajectory leading from x' to x while \mathcal{B}_t , kl_t , and Θ_t are defined as in Eq. (14). Skipping a more mathematical derivation of Eq. (22) we only point the analogy with the well known Green's function of a free particle G_0 in one-dimension $G_0 = (2ik)^{-1}e^{i|x-x'|}$. Eq. (22) simply generalizes this expression by adding the additional paths from x' to x which are due to the multiply connected nature of the graph.

Let us now consider the specific matrix elements $G_{jj'}$ of the Green's function Eq. (22), which appear in the definition of the reaction matrix Eq. (19). It is our goal to represent them in terms of the scattering trajectories contributing to the S-matrix element $S_{jj'}$ according to Eq. (14). To this end we note that the contribution of each trajectory is the same in the two expressions up to an overall factor $(2ik)^{-1}$ appearing in the Green's function. However, the set of contributing trajectories is different: in the open system we have $\rho^{(j)} = 0$ meaning that no backscattered trajectories from the auxiliary vertices $1 \leq j \leq M$ contribute, while in the closed graph such trajectories do exist. In order to get their contributions also from Eq. (14) we consider multiple scattering at the graph with scattering trajectories reinjected an arbitrary number of times. Then it becomes indeed possible to represent all trajectories inside the closed graph as combinations of scattering trajectories and we find

$$G_{jj'} = (2ik)^{-1} \left(2\delta_{jj'} + 4 \sum_{n=1}^{\infty} (S^n)_{jj'} \right), \quad (23)$$

where n counts the multiple scattering at the graph. The first term ($n = 0$) corresponds to the zero-length trajectories from j to j . Note that $G_{jj'}$ actually denotes the limit of $G(x, x'; k)$ as $x \rightarrow j$ and $x' \rightarrow j'$ and that there are always two options to reach a point in the vicinity of a vertex j : with or without preceding scattering at this vertex. Combining these options for j and j' gives the prefactor 4 (2 for $n = 0$) in Eq. (23). After summing the geometric series in Eq. (23) we arrive at Eq. (20).

Not only have we established in this way an analogue of the well known reaction-matrix formalism for quantum graphs, we have also given the first semiclassical interpretation of this theory: our derivation of Eq. (20) was entirely based on comparing the contributions of classical trajectories summing to an S-matrix element or Green's function, respectively.

In Fig. 1 we demonstrate numerically, how Eq. (21) can be used to compute the S-matrix of a scattering graph from its corresponding closed analogue. For the tetrahedron graph (see figure) we computed the lowest 500 eigenvalues and eigenfunctions and using Eqs. (18), (21) we obtain an approximation for the S-matrix of the graph (see circles). For simplicity we consider the case $M = 1$ where the S-matrix reduces to a single phase. The resulting data are in excellent agreement with the exact result (solid line) calculated from Eq. (12). We verified that the comparison is equally successful for multiple leads and other types of graphs.

We continue by deriving the effective Hamiltonian for a quantum graph. To this end we rewrite Eq. (19) in the standard form

$$K_{jj'} = \pi \sum_{n=1}^{\infty} W_{n,j}^* \frac{I}{k^2 - k_n^2} W_{n,j'}, \quad (24)$$

where

$$W_{n,j}(k) = \sqrt{k/\pi} \psi_{n,j} \quad (25)$$

denotes the coupling of the internal level n to the scattering lead j . We see from Eq. (25) that these coupling constants are proportional to the internal eigenfunction at the point where the lead is attached, as it should be expected. Following [28] we can now use some algebra to rewrite Eq. (21) in the form

$$S = I - 2\pi i W^\dagger \frac{I}{E - \mathcal{H}} W, \quad (26)$$

where the S-matrix is expressed in terms of an effective Hamiltonian \mathcal{H} , which has in the eigenbasis of the graph the matrix elements

$$\mathcal{H}_{nn'} = k_n^2 \delta_{nn'} - i\pi (WW^\dagger)_{nn'}. \quad (27)$$

Note that this Hamiltonian depends on energy via Eq. (25). Whenever this dependence can be neglected, Eq. (27) can be diagonalized to find the resonance poles. In this regime, the predictions of RMT for the statistical properties of the resonances [26, 27, 28] are applicable.

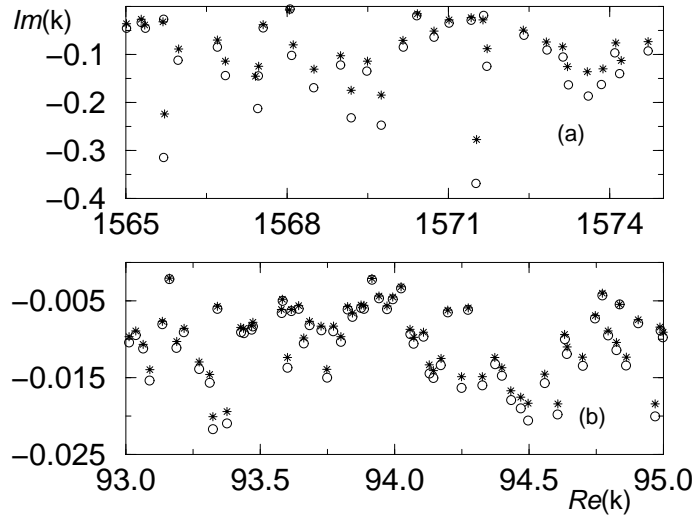


Figure 2. Poles of the $S^{(V)}$ -matrix for regular Neumann graphs. The exact evaluated poles are indicated with (o) while (*) are the results of the perturbation theory (31): (a) $V = 5$ and $v = 4$ and (b) $V = 15$ and $v = 14$.

5. Statistical properties of resonance widths

One of the basic concepts in the quantum theory of scattering are the resonances. They represent long-lived intermediate states to which bound states of a closed system are converted due to coupling to continua. On a formal level, resonances show up as poles of the scattering matrix $S^{(M)}$ occurring at complex wave-numbers $\kappa_n = k_n - \frac{i}{2}\Gamma_n$, where k_n and Γ_n are the position and the width of the resonances, respectively. From (12) it follows that the resonances are the complex zeros of

$$\zeta_{\tilde{\mathcal{G}}}(\kappa) = \det(\mathbf{1} - \tilde{S}_B(\kappa; A)) = 0. \quad (28)$$

The eigenvalues of $\tilde{S}_B = D(k; A)\tilde{R}$ are in the unit circle, and therefore the resonances appear in the lower half of the complex κ plane.

One important parameter that is associated with the statistical properties of resonance widths is the Ericson parameter defined through the scaled mean resonance width as:

$$\langle \gamma \rangle_k \equiv \left\langle \frac{\Gamma}{\Delta} \right\rangle_k \quad (29)$$

where $\langle \cdot \rangle_k$ denotes spectral averaging and Δ is the mean spacing between resonances. The Ericson parameter defines whether the resonances are overlapping ($\langle \gamma \rangle_k > 1$) or isolated ($\langle \gamma \rangle_k < 1$).

For relatively small values of the Ericson parameter a perturbation theory can be carried out in order to evaluate the resonance widths. Indeed, the difference $\delta R = R - \tilde{R}$ gets smaller as larger graphs are considered (for graphs with Neumann boundary conditions it is easy to see that the difference is of order $\frac{1}{v}$). That is, the leads are weakly coupled to the compact part of the graph. To lowest order, ($\delta R = 0$), the resonances

coincide with the spectrum of the compact graph. Let k_n be in the spectrum. Hence, there exists a vector $|n\rangle$ which satisfies the equation

$$D(k_n)R|n\rangle = 1|n\rangle. \quad (30)$$

To first order in δR , the resonances acquire a width

$$\delta\kappa_n = -i \frac{\langle n|D(k_n)\delta R|n\rangle}{\langle n|L|n\rangle}. \quad (31)$$

The above equation shows clearly that the formation of resonances is closely related to the internal dynamics inside the scattering region which is governed by \tilde{S}_B .

To check the usefulness of Eq. (31), we searched numerically for the true poles for a few scattering graphs and compared them with the approximation (31). In Fig. 2 we show the comparison for fully connected Neumann graphs with $V = 5, 15$ and $A = 0$. As expected the agreement between the exact poles and the perturbative results improves as v increases.

5.1. Resonance width distribution

An important feature of the distribution of the resonances in the complex plane can be deduced by studying the secular function $\zeta_{\tilde{g}}(\kappa)$. Consider $\zeta_{\tilde{g}}(\kappa = 0)$. If one of the eigenvalues of the matrix \tilde{R} (9) takes the value 1, $\zeta_{\tilde{g}}(k = 0) = 0$ and because of the quasi-periodicity of $\zeta_{\tilde{g}}$, its zeros reach any vicinity of the real axis infinitely many times. For v -regular Neumann graphs without magnetic vector potential ($A = 0$) the matrix \tilde{R} has indeed an eigenvalue 1, and therefore the distribution of resonance widths is finite in the vicinity of $\gamma = 0$ for these systems. For generic graphs, the spectrum of \tilde{R} is typically inside a circle of radius $\mu_{max} < 1$. This implies that the poles are excluded from a strip just under the real axis, whose width can be estimated by

$$\Gamma_{gap} = -2 \ln(|\mu_{max}|) / L_{max}, \quad (32)$$

where L_{max} is the maximum bond length. The existence of a gap is an important feature of the resonance width distribution $\mathcal{P}(\gamma)$ for chaotic scattering systems.

A similar argument was used recently in [24] in order to obtain an *upper* bound for the resonance widths. It is

$$\Gamma_{max} \sim -2 \ln(|\mu_{min}|) / L_{min}, \quad (33)$$

where μ_{min} and L_{min} are the minimum eigenvalue and bond length, respectively.

The distribution of the complex poles for a generic fully connected graph with $V = 5$ is shown in Fig 3a. The vertical line which marks the region from which resonances are excluded was computed using (32).

Random matrix theory can provide a general expression for the distribution of resonances. Specifically, Fyodorov and Sommers [27, 28] proved that the distribution of scaled resonance widths for the unitary random matrix ensemble, is given by

$$\mathcal{P}(\gamma) = \frac{(-1)^M}{\Gamma(M)} \gamma^{M-1} \frac{d^M}{d\gamma^M} \left(e^{-\gamma\pi g} \frac{\sinh(\gamma\pi)}{(\gamma\pi)} \right), \quad (34)$$

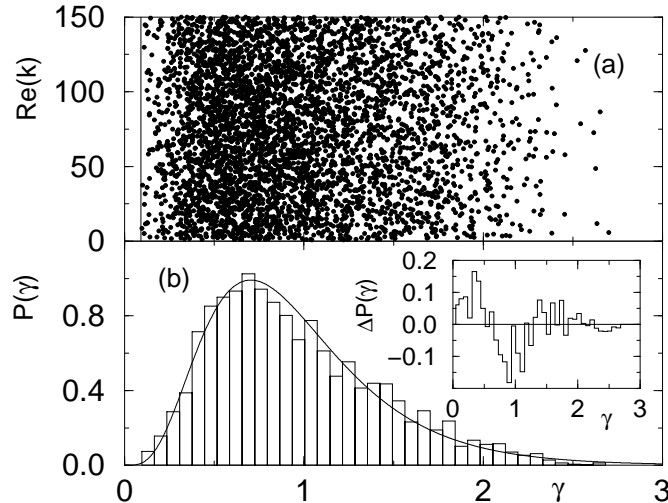


Figure 3. (a) The 5000 resonances of a single realization of a complete $V = 5$ graph with $A \neq 0$ and $M = V$. The solid line marks the position of the gap γ_{gap} . (b) The distribution of resonance widths $\mathcal{P}(\gamma)$. The solid line is the RMT prediction (34). The difference $\mathcal{P}(\gamma) - \mathcal{P}_{CUE}(\gamma)$ is shown in the inset.

where the parameter $g = \frac{2}{(1 - \langle S^D \rangle_k^2)} - 1$ controls the degree of coupling with the channels (and it is assumed that $g_i = g \forall i = 1, \dots, M$).

In the limit of $M \gg 1$, Eq. (34) reduces to the following expression [28]

$$\mathcal{P}(\gamma) = \begin{cases} \frac{M}{2\pi\gamma^2} & \text{for } \frac{M}{\pi(g+1)} < \gamma < \frac{M}{\pi(g-1)} \\ 0 & \text{otherwise} \end{cases}. \quad (35)$$

It shows that in the limit of large number of channels there exists a strip in the complex κ - plane which is free of resonances. This is in agreement with previous findings [35, 36, 37]. In the case of maximal coupling i.e. $g = 1$, the power law (35) extends to infinity, leading to divergencies of the various moments of γ 's. Using (34) we recover the well known Moldauer-Simonius relation [36] for the mean resonance width [28]

$$\langle \gamma \rangle_k = -\frac{\sum_{i=1}^V \ln(|\langle S^D \rangle_k|^2)}{2\pi}. \quad (36)$$

The resonance width distribution for a $V = 5$ regular and generic graph is shown in Fig. 3b together with the RMT prediction, which reproduces the numerical distribution quite well. Fig. 4 shows a similar comparison for Neumann graphs. In this case, a clear deviation from the RMT prediction is observed. The main feature of $\mathcal{P}(\gamma)$ is the relatively high abundance of resonances in the vicinity of the real axis which is of dynamical nature and conforms with the expectations (see related discussion above Eq. (32)).

Although the absence of a gap in a strict sense is apparent in all the Neumann graphs that we have studied, still one can speak about a gap in a ‘‘probabilistic’’ sense. To show this, we have calculated the ratio of the resonance width standard deviation

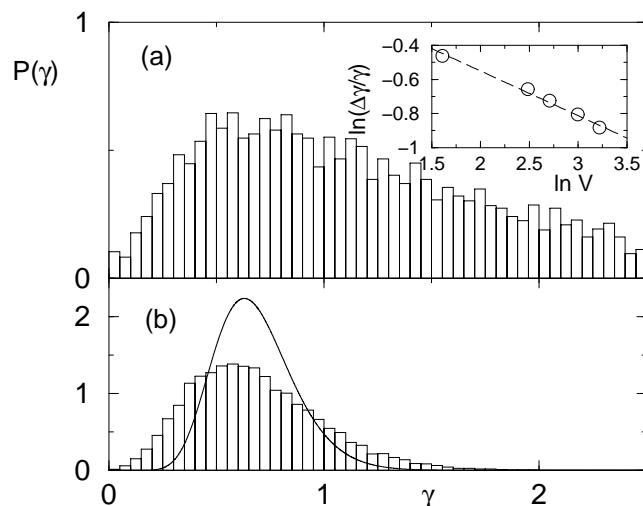


Figure 4. (a) Resonance width distribution $\mathcal{P}(\gamma)$ for fully connected Neumann graphs with (a) $A = 0$ and $M = V = 5$; (b) $A \neq 0$ and $M = V = 15$. The solid line is the RMT prediction (34). In the inset we report the relative ratio $\frac{\Delta\gamma}{\langle\gamma\rangle_k}$ vs. V for fully connected graphs with $A = 0$. As V increases, the distribution is concentrated more around its mean value and an effective gap is created. The dashed line has slope -0.25 and is the best fit to the numerical data.

$\Delta\gamma$ with respect to the mean resonance width $\langle\gamma\rangle_k$ for various fully connected graphs. Our numerical data reported in the inset of Fig. 4 for various values of V suggest that $\frac{\Delta\gamma}{\langle\gamma\rangle_k} \sim \frac{1}{V^\alpha}$ with $\alpha \simeq 0.25$.

For $g \gg 1$ (i.e. weak coupling regime) Eq. (34) reduces to the following expression

$$\mathcal{P}(\gamma) = \frac{(\beta M/2)^{\beta M/2}}{\langle\gamma\rangle_k \Gamma(\beta M/2)} \left(\frac{\gamma}{\langle\gamma\rangle_k} \right)^{\beta M/2 - 1} \exp(-\gamma \beta M/2 \langle\gamma\rangle_k), \quad (37)$$

where $\beta = 1(2)$ for systems which respect (break) time-reversal symmetry, and $\Gamma(x)$ is the Gamma-function. We notice that (37) is the so-called χ^2 distribution and can be derived independently using simple perturbation theory [38].

A simple graph that satisfy the weak coupling limit is the Neumann star graph. They consist of v_0 bonds and one lead, all of which emanate from a single common vertex labeled with the index $i = 0$. It is a simple matter to derive the scattering matrix $S^{(M=1)}$ which is reduced to a single phase factor [23]

$$S(k) \equiv e^{i\phi(k)} = \frac{-\sum_{i=1}^{v_0} \tan(kL_i) + i}{+\sum_{i=1}^{v_0} \tan(kL_i) + i} \quad (38)$$

In Fig. 5 we present our numerical results for $\mathcal{P}(\gamma)$ for a star graph with $v_0 = 20$. The data are in excellent agreement with the RMT expectation given in Eq. (38). We point out that in this case the coupling to the continuum is weak since $g \simeq 10 \gg 1$ and therefore the χ^2 -distribution with $M = 1$ is applicable.

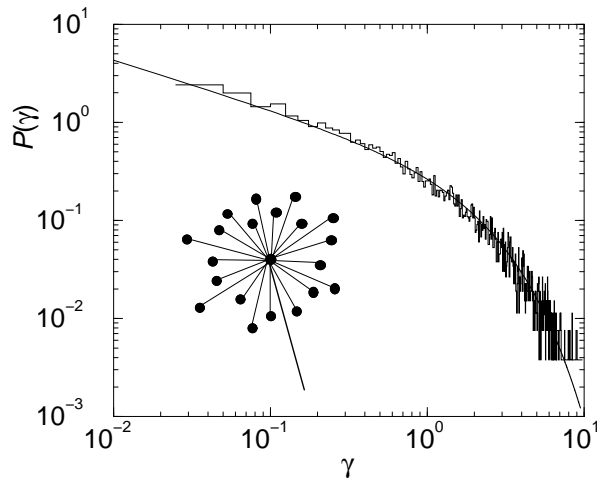


Figure 5. The rescaled resonance width distribution $\mathcal{P}(\gamma)$ for a star graph with $v_0 = 20$ (inset). The solid line is the RMT prediction Eq. (37).

5.2. Resonance-trapping in graphs

As mentioned at the end of Section 4.2, the effective Hamiltonian Eq. (27) is in general an infinite-dimensional and energy-dependent matrix and thus very hard to treat. However, there are situations where this Hamiltonian can be approximated with good accuracy by a finite and constant matrix. For example, this is the case, when the energy levels of the closed system are clustered, e. g. by an underlying shell or band structure.

Let us calculate under this assumption the Ericson parameter Eq. (29) of a group of N resonances of a graph at large $k \gg \Delta$. The resonances can be found by diagonalizing \mathcal{H} . From Eq. (27) we have for graphs with Neumann b. c.

$$\begin{aligned}
 \langle \gamma \rangle_N &= -\frac{1}{kN\Delta} \text{Im tr } \mathcal{H} \\
 &= \frac{\pi}{kN\Delta} \sum_{n,j} |W_{n,j}|^2 \\
 &= M \frac{\langle |\psi_{n,j}|^2 \rangle}{\Delta}.
 \end{aligned} \tag{39}$$

Note that diagonalization of \mathcal{H} yields the resonances in the complex energy plane, while we are interested in the wavenumber κ . This was accounted for in the first line of Eq. (39). From the normalization of the eigenfunctions of the graph we deduce that the mean intensity of an eigenstate is the inverse of the total length \mathcal{L} of the graph $\langle |\psi_{n,j}|^2 \rangle = \mathcal{L}^{-1}$. Hence, if Δ was equal to the mean level spacing of all levels, π/\mathcal{L} , the Ericson parameter would be fixed to $\langle \gamma \rangle_N \sim M/\pi$. However, we said above that the effective Hamiltonian can be used only if there is clustering of levels, meaning that the local mean spacing inside the cluster of N resonances is $\Delta \ll \pi/\mathcal{L}$. Therefore we have in such a situation not only $\langle \gamma \rangle_N \gg 1$ but even $\gamma \gg M$.

Theoretical calculations, based on RMT modeling, predict that in this situation the statistical properties of the resonances change drastically: with increasing strength

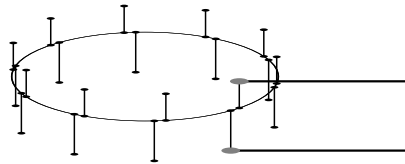


Figure 6. Ring-shaped periodic graph with $N = 10$ unit cells.

of the coupling, M very broad resonances are formed, whereas the remaining $N - M$ approach the real axis and become long lived (trapped) [37, 39]. This counterintuitive phenomenon, which was recently demonstrated in experiments on microwave resonators [40] is called “resonance trapping”.

Let us now illustrate this phenomenon for the case of quantum graphs. To this end we use a graph model consisting of N identical unit cells forming a periodic ring as shown in Fig. 6 (we note that our numerical data were already included in the recent review by Dittes [33]). Each unit cell consists of four vertices. Two of these vertices are T -shaped junctions with Neumann b. c. ($\lambda = 0$). The other two are dead ends where we impose Dirichlet b. c. ($\lambda = \infty$). In one of the unit cells the dead ends have variable boundary conditions $0 \leq \lambda_{\text{leads}} \leq \infty$ and are connected to a scattering channel. As long as the coupling to the channels is zero ($\lambda = \infty$ at all dead ends), the spectrum is organized in discrete bands, each containing N eigenvalues. These eigenvalues are seen in Fig. 7 as intersections of the solid lines with the real axis. We observe that the spacing within the bands can indeed be much smaller than the spacing between the bands.

As soon as λ_{leads} is finite, the eigenstates of the closed system are turned into resonances with a finite lifetime. In Fig. 7 we show the motion of resonances in the complex κ -plane as we increase the coupling constant of the system by decreasing λ_{leads} to zero. One can clearly see the resulting redistribution of the S -matrix poles. For particularly narrow bands, e. g. at $k \sim 4.2$, we observe indeed two broad resonances with a width several orders of magnitude above that of the remaining poles, while for the broader bands at least one broad resonance can be distinguished.

6. Conclusions

Quantum graphs are used in our days as a paradigmatic model of quantum chaos. By connecting them with infinite leads one turns them into scattering systems. As a result, a scattering formalism can be developed, and an exact expression for the scattering matrix can be found.

Due to the relative ease by which a large number of numerical data can be computed for the graph models, we have performed a detailed statistical analysis of resonance widths. A gap for the resonance widths has been obtained for “generic” graphs and its absence was explained for Neumann graphs. Finally, we have shown that the

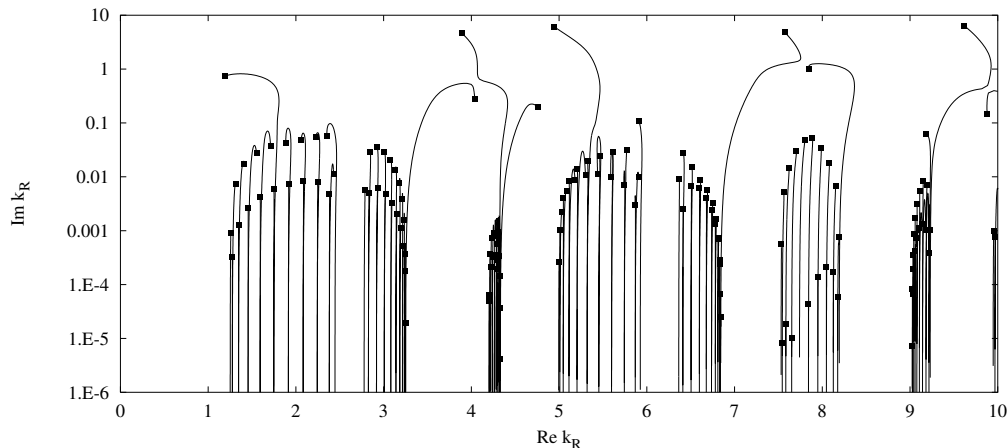


Figure 7. Trajectories in the complex κ -plane of the resonances of a ring graph with $N = 20$ unit cells as λ_{leads} falls from ∞ to 0. For the maximum coupling to the two attached scattering channels ($\lambda_{\text{leads}} = 0$), the location of the resonances is marked by squares.

phenomenon of resonance trapping can appear also in quantum graphs.

7. Acknowledgments

We would like to express our gratitude to Prof. Uzy Smilansky to whom we owe our interest in the subject and who contributed a great deal to most results discussed in this paper. We also acknowledge many useful discussions with Y. Fyodorov, A. Ossipov and M. Weiss. (T. K) acknowledges support by a Grant from the GIF, the German-Israeli Foundation for Scientific Research and Development.

- [1] S. Alexander, Phys. Rev. B **27**, 1541 (1985).
- [2] C. Flesia, R. Johnston and H. Kunz, Europhys. Lett. **3**, 497 (1987).
- [3] R. Mitra and S. W. Lee, *Analytical techniques in the theory of guided waves*, Macmillan, New York.
- [4] P. W. Anderson, Phys. Rev. B **23**, 4828 (1981); B. Shapiro, Phys. Rev. Lett. **48** 823 (1982).
- [5] J. T. Chalker and P. D. Coddington, J. Phys. C **21**, 2665 (1988); Rochus Klesse and Marcus Metzler, Phys. Rev. Lett. **79**, 721 (1997); R. Klesse, Ph. D. Thesis, Universitat zu Köln, AWOS-Verlag, Erfurt, 1996.
- [6] Y. Avishai, J. M. Luck, Phys. Rev. B **45**, 1074 (1992); T. Nakayama, K. Yakubo, R. L. Orbach, Rev. Mod. Phys. **66**, 381 (1994).
- [7] Y. Imry, *Introduction to Mesoscopic Systems*, Oxford, New York (1996); D. Kowal, U. Sivan, O. Entin-Wohlman, Y. Imry, Phys. Rev. B **42**, 9009 (1990).
- [8] J. Vidal, G. Montambaux, D. Doucot, Phys. Rev. B **62**, R16294 (2000).
- [9] Zhang et al. Phys. Rev. Lett. **81**, 5540 (1998).
- [10] Colin de Verdière. *Spectres de Graphes*. Société Mathématique de France, Marseille (1998).
- [11] P. Exner, Phys. Rev. Lett. **74**, 3503 (1995); P. Exner, P. Seba, Rep. Math. Phys. **28**, 7 (1989); J. E. Avron, P. Exner, Y. Last, Phys. Rev. Lett. **72**, 896 (1994); R. Carlson, Electronic Journal of Differential Equations **6**, 1 (1998).
- [12] Jean-Pierre Roth, in: *Lectures Notes in Mathematics: Theorie du Potentiel*, A. Dold and B. Eckmann, eds. (Springer-Verlag) 521-539.

- [13] Tsampikos Kottos and Uzy Smilansky. Phys. Rev. Lett. **79**, 4794 (1997).
- [14] Tsampikos Kottos and Uzy Smilansky, Annals of Physics **274**, 76 (1999).
- [15] Akkermans E, Comtet A, Desbois J, Montambaux G, Texier C, Annals of Physics **284**, 10 (2000).
- [16] Berkolaiko G. and Keating J. Phys. A **32** 7827 (1999); Berkolaiko G., Bogomolny E.B., and Keating J. Phys. A **34** 335 (2001).
- [17] H. Schanz and U. Smilansky. Phys. Rev. Lett. **84**, 1427 (2000); Phil. Mag. B **80**, 1999 (2000);
- [18] G. Tanner, J. Phys. A **33**, 3567 (2001).
- [19] T. Kottos and H. Schanz, Physica E **9**, 523 (2001).
- [20] G. Berkolaiko, H. Schanz, R. S. Whitney, Phys. Rev. Lett. **88**, 104101 (2002).
- [21] F. Barra, P. Gaspard, J. Stat. Phys. **101**, 283 (2000); F. Barra, P. Gaspard, Phys. Rev. E **63**, 066215 (2001).
- [22] L. Kaplan, Phys. Rev. E **64**, 036225 (2001).
- [23] Tsampikos Kottos and Uzy Smilansky, Phys. Rev. Lett. **85**, 968 (2000); J. Phys. A, to appear (2003).
- [24] F. Barra and P. Gaspard, Phys. Rev. E, **65**, 016205 (2002).
- [25] C. Texier and G. Montambaux, J. Phys. A **34** 10307 (2001); C. Texier, J. Phys. A **35** 3389 (2002).
- [26] Y. V. Fyodorov and H.-J. Sommers, Phys. Rev. Lett. **76**, 4709 (1996); Y. V. Fyodorov, D. V. Savin, and H.-J. Sommers, Phys. Rev. E **55** R4857 (1997).
- [27] H-J Sommers, Y. V. Fyodorov, and M. Titov, J. Phys. A: Math. Gen. **32** L77 (1999); Y. Fyodorov, H-J Sommers, Pis'ma Zh. Eksp. Teor. Fiz. **63** 970 (1996) [JETP Lett. **63**,1026 (1996)]
- [28] Y. Fyodorov, H-J Sommers, J. Math. Phys. **38** 1918 (1997); P. Mello in *Les Houches Summer School on Chaos and Quantum Physics*, E. Akkermans et.al., eds (North-Holland) 437-491 (1994).
- [29] P. Exner, P. Seba, Rep. Math. Phys. **28**, 7 (1989); P. Exner, J. Phys. A: Math. Gen. **29**, 87 (1996).
- [30] E. P. Wigner and L. Eisenbud, Phys. Rev. **72**, 29 (1947).
- [31] H. Feshbach, *Theoretical Nuclear Physics*, Wiley-Interscience, 1992.
- [32] C. Mahaux and H. A. Weidenmüller, *Shell-Model Approach to Nuclear Reactions*, North Holland, Amsterdam, 1969.
- [33] F. M. Dittes, Phys. Rep. **339**, 215 (2000).
- [34] K. Pichugin, H. Schanz, and P. Šeba, Phys. Rev. E **64**05, 056227 (2001).
- [35] P. Gaspard, in "*Quantum Chaos*", *Proceedings of E. Fermi Summer School 1991*, G. Casati et. al., eds. (North-Holland) 307; P. Gaspard and S. A. Rice, J. Chem Phys **90**, 2225,2242,2255(1989); **91** E3279, (1989).
- [36] P. A. Moldauer, Phys. Rev. C **11**, 426 (1975); P. A. Moldauer, Phys. Rep. **157**, 907 (1967); M. Simonius, Phys. Lett. **52B**, 279 (1974).
- [37] V. Sokolov and G. Zelevinsky, Phys. Lett. B **202** 10 (1988); E. Sobeslavsky, F. M. Dittes, and I. Rotter, J. Phys. A: Math. Gen. **28**, 2963 (1995).
- [38] R. A. Jalabert, A. D. Stone and Y. Alhassid, Phys. Rev. Lett. **68**, 3468 (1992).
- [39] F. Haake, F. Izrailev, N. Lehmann, D. Saher, H-J Sommers, Z. Phys. B **88**, 359 (1992); N. Lehmann, D. Saher, V. Sokolov, H-J Sommers, Nucl. Phys. A **582**, 223 (1995).
- [40] E. Persson, I. Rotter, H.-J. Stöckmann, and M. Bath, Phys. Rev. Lett. **85**, 2478 (2000).